

3-D Computation of Surface Sputtering and Redeposition Due to Hall Thruster Plumes

J. M. Fife, M. R. Gibbons, and W. A. Hargus
U.S. Air Force Research Laboratory
Edwards AFB, CA

D. B. VanGilder and D. E. Kirtley
ERC, Inc.
Edwards AFB, CA

L. K. Johnson
Jet Propulsion Laboratory
Pasadena, CA

A 3-D computational plasma interaction modeling system is being developed to predict the interaction of electric propulsion plumes with surfaces. The system, named COLISEUM, is designed to be flexible, usable, and expandable, allowing users to define surfaces with their choice of off-the-shelf 3-D solid modeling packages. These surfaces are then loaded into COLISEUM, which calculates plasma expansion from electric thrusters using a variety of functional modules. Functional modules are interchangeable, and can range from simple (collisionless ray tracing) to complex (PIC-DSMC). Surface interaction parameters such as ion flux, ion energy, sputtering, and re-deposition are computed. Using the simplest functional modules, runs can be set up, executed and analyzed in less than 8 hours. Development to date has progressed to include two functional modules: PRESCRIBED_PLUME, which imports and superimposes a plume distribution, and RAY, which performs ray tracing of flux from point sources. This paper presents a new COLISEUM algorithm for calculating equilibrium re-sputtering and re-deposition of materials. This algorithm enables calculation of net deposition and sputtering of surfaces inside HET test facilities as well as in the space environment. Two cases are presented – one for a laboratory experiment in which sputtering and redeposition were measured on Kapton samples, and another in which sputtering and redeposition on a generalized geosynchronous spacecraft is predicted.

Introduction

Several EP devices are currently being evaluated for use onboard U.S. commercial and military spacecraft. One of the most promising for near-term use is the Hall-effect thruster (HET). Over 120 HETs have flown on Russian spacecraft, where typical flight units have specific impulses around 1600 seconds and efficiencies near 50%.¹ HETs operate by generating a stationary xenon plasma inside an annular channel. Strong radial magnetic fields are applied which impede electron motion, but allow ions to accelerate axially out of the device with velocities around 20 km/s (energies of around 300 eV).

High-energy HET exhaust ions may erode (sputter) surfaces on which they impinge. In addition, this sputtered material may be re-deposited on other spacecraft surfaces. These issues, and others, such as electromagnetic interference and spacecraft charging, cause some concern for spacecraft designers who want the maneuverability EP offers but do not want increased risk.

Efforts are underway to accurately quantify some of the risks associated with integration of EP with spacecraft, including

surface erosion and re-deposition. Work has been done to computationally model expansion of HET plumes.² Additionally, Gardner et al. have developed Environment Work Bench (EWB), a program that calculates sputtering of spacecraft surfaces by superimposing pre-computed EP plumes onto spacecraft geometries.^{3,4} However, existing programs do not self-consistently calculate the plume expansion with 3-D surface sputtering in a usable, flexible way.

The Air Force Research Laboratory is leading development of a new software package named COLISEUM, which will be capable of self-consistently modeling plasma propagation and interactions with arbitrary 3-D surfaces. Three important requirements have been placed on COLISEUM: It must be USABLE, FLEXIBLE, and EXPANDABLE.

USABLE means a typical engineer is able to set up and run a typical low-fidelity case in less than one day with less than three days training.

FLEXIBLE means COLISEUM is able to simulate at least three important cases: a) a single spacecraft, b) multiple spacecraft in formation, and c) laboratory conditions (e.g. the

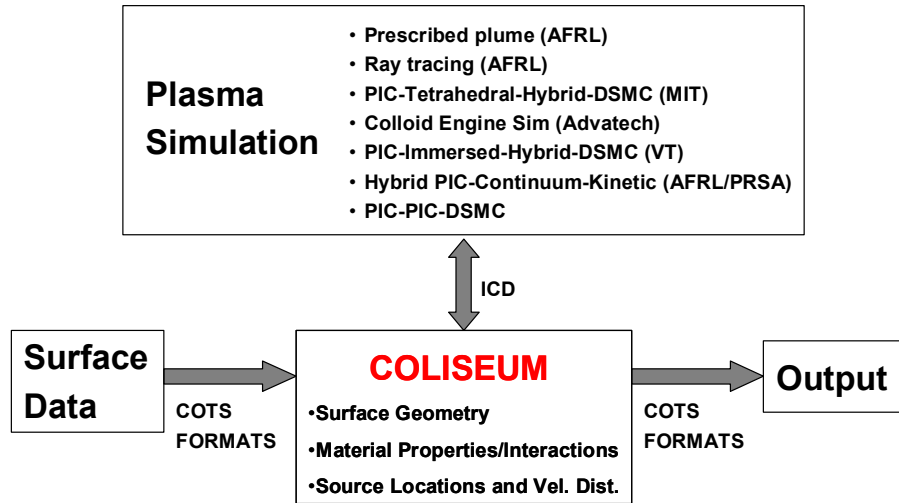


Fig. 1 Architecture for using various interchangeable plasma simulation techniques with the same 3-D surface geometry.

interior of a vacuum test facility). Simulating laboratory conditions is very important for two reasons. First, since there is very little on-orbit data for EP thrusters, ground-based tests must be relied upon for the bulk of code validation. Second, by modeling the laboratory conditions, COLISEUM can help engineers interpret lab measurements.

In addition to being able to simulate multiple geometries, COLISEUM is flexible in its use of plasma simulation algorithms. Problem set-up and geometry definition is performed once. Then, the user may select from a set of interchangeable plasma simulation algorithms to perform the solution. If fast execution is desired, a low-fidelity technique can be selected such as ray tracing. For higher fidelity (at the cost of longer run-time), something like Particle-In-Cell (PIC) can be used.

EXPANDABLE means COLISEUM can be easily expanded to incorporate new plasma simulation algorithms, new capabilities, or improved efficiency. Furthermore, as new plasma simulation algorithms are added, old ones will continue to function.

Approach

Fig. 1 shows how the COLISEUM Application Programming Interface (API) works with a set of various interchangeable plasma simulations (applications). In general, the COLISEUM API can be viewed as a framework in which 3-D plasma simulations can be quickly integrated. Common calculations (such as those related to surfaces, material properties, and flux sources) are standardized, grouped, and provided as a resource library (data and subroutines) to each simulation. This resource library takes the form of a `.lib` file that users link with their set of plasma simulation routines.

Plasma simulation modules are the primary functional components of COLISEUM. They calculate plasma

propagation of matter on the volume domain. They contain algorithms, such as ray tracing, fluid, PIC, DSMC, or hybrids thereof, which perform a solution subject to pre-set boundary conditions. Plasma simulation modules are interchangeable. They all conform to the COLISEUM API which is formalized in the Interface Control Document (ICD).

The COLISEUM resource library functions support tasks common to all types of plasma simulations. They handle boundary conditions, and provide support to plasma simulation modules.

The purpose of this modular design is to give COLISEUM flexibility and expandability. A large number of plasma simulation modules are desired to allow flexibility in solving a variety of different problems. The ICD is, therefore, very important, because it describes for authors of plasma simulation modules a) what inputs and boundary conditions must be recognized, b) what outputs are expected, and c) what COLISEUM resource functions are available. The ICD and COLISEUM resource library may be distributed to outside groups so that COLISEUM can be expanded through addition of new plasma simulation modules.

Surfaces

Surfaces are modeled in finite-element fashion as contiguous triangular elements joined at the vertices (nodes). COLISEUM does not generate 3-D geometries or surfaces; instead, it imports them from other software.

Users create custom geometries using almost any mainstream commercial 3-D solid modeling package. Then, they use finite element analysis software to mesh the surface of their geometry as if they were going to perform a structural analysis using thin shells. The user then saves the meshed surface file in ANSYS format, which is readable by COLISEUM. ANSYS finite element format was chosen because it is widely supported by finite element packages.

This concept of separating the surface geometry definition from the plasma calculation has proven very successful. It greatly reduced development time and cost by eliminating the need for a separate surface definition module. It allows users to choose which software to use in defining geometries. And, users can import into COLISEUM geometries that have already been defined for other reasons (structural, thermal, etc.).

Surface Properties

The user may provide three databases in conjunction with a surface geometry: a component database, a material database, and a material interaction database.

The component database associates specific surfaces with component names and material names. These associations are established by using a component number which is specified in the ANSYS file using integer values in the elastic modulus field. For example, the component database may specify component number 34 as component name "north_solar_cell" and material "quartz."

The material database associates component names with material names and material properties. The plasma simulations RAY and PRESCRIBED_PLUME require, in addition to material name, molecular weights, and charges (in the case of ions).

The material interaction database contains the sputter yield coefficients and sticking coefficients of one material interacting with the other, e.g. between Xe^+ and Kapton.

Sources

Sources are modeled as having a specific velocity distribution, $f_s(\vec{r}, \vec{v}, t)$, that is a function of position on the surface, of three-dimensional velocity space, and of time:

$$\dot{m}_s = \iint_{S_V} f_s(\vec{r}, \vec{v}, t) d^3v ds \quad (1)$$

Rather than specify $f_s(\vec{r}, \vec{v}, t)$ directly, however, three COLISEUM resource library functions are provided for each source type. These a) give the distribution of velocities at some point P in space due to the source, b) provide a random sample from the source velocity distribution at the surface, or c) update the source to be valid at some new time, t .

This method is extremely descriptive and general. Plasma simulation modules may use the three source functions to treat the source distribution function in various ways. For example, using the first function, a plasma simulation module can be written to treat the source element as a source for geometric ray tracing. Alternately, particle methods can use the second sample from the velocity distribution and introduce particles randomly over the full element surface. Therefore, this choice of source definition methods gives COLISEUM great flexibility by enabling a wide variety of plasma simulation techniques with the same source definition.

A set of pre-defined source types (Hall thruster, mono-energetic, half-Maxwellian, etc. have been written and

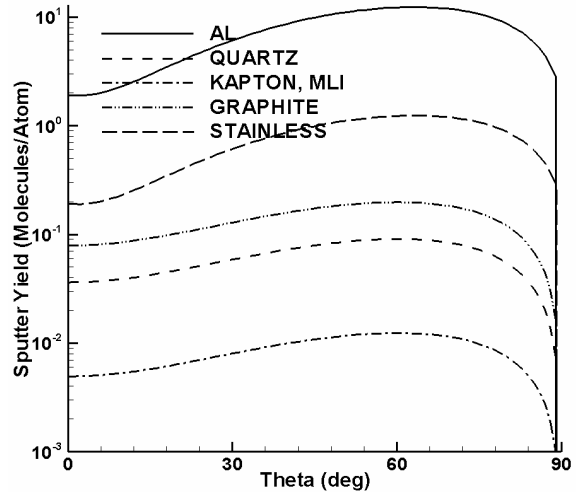


Fig. 2. Models of sputter yield versus incidence angle for Xe^+ at 300eV.

implemented in the COLISEUM resource library. In addition, users may add their own user-defined source type (which must be coded and linked with the COLISEUM resource library).

Plasma Simulation

Currently, two modules have been written and tested at AFRL. The first, PRESCRIBED_PLUME, allows the user to import a previously calculated or measured plume field. This plume is superimposed over the user's surface geometry. Plasma densities, fluxes, and sputter rates are then calculated at each surface node.

The second module, RAY, uses ray tracing to calculate the flux from all sources onto all surface nodes. Once again, density, flux, and sputter rate are calculated.

Modules under development at AFRL and other institutions are incorporating statistical kinetic methods for plasma calculation such as PIC and DSMC. Some of these methods also use unstructured meshes, adaptive meshes, and domain decomposition. Primarily, these techniques will be incorporated to add flexibility to the simulation. For instance, domain decomposition will allow the domain to be broken into smaller sub-domains, each potentially having different algorithms, depending on local parameters as the Debye length or mean free path.

Sputtering and Redeposition

The material interaction database can support multiple surface sputtering models. Currently, three models are implemented: a) constant yield, b) a model by Roussel et al.⁵ (also used by Gardner et al.³), and c) a model by Kannenberg⁶. In this paper, sputtering is modeled for Xe^+ on Aluminum, quartz, Kapton, multi-layer insulation (MLI), graphite and stainless steel. For these materials, models by Roussel and Kannenberg are used. For the Kannenberg models the assumptions are: a peak yield at 60 degrees, linear energy dependence, zero threshold, and a ratio of peak yield to yield

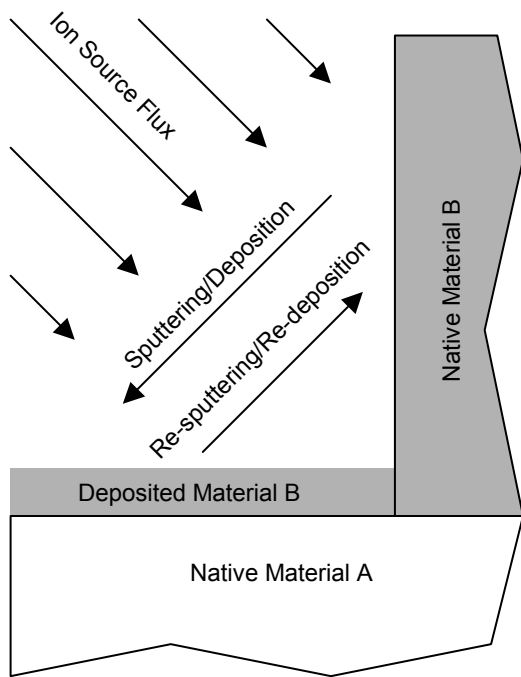


Fig. 3. Illustration of sputtering, deposition, re-sputtering, and re-deposition for a simple geometry with two materials: material A and B, where material B has higher sputter yield than material A.

at normal incidence of 2.5. The ratio 2.5 is taken as an average from models and experiments collected by Boyd and Falk.⁷ The yield at normal incidence for Kapton was taken from measurements performed at NASA: 0.005 units/ion.⁸ The yield at normal incidence for Graphite, .08 units/ion, is taken from Rosenberg and Wehner.⁹ Fig. 2 shows the sputter yield versus incidence angle at 300eV. Yield of MLI was assumed to be identical to Kapton, since data was not available. The yield of quartz was taken from sputter measurements during an SPT-140 test, even though solar cell cover glasses were used instead of quartz.⁸ Yield for stainless steel and aluminum (AL) was scaled linearly with energy from yields of iron and aluminum, due to Argon at 500eV. The uncertainty in yield of stainless steel and aluminum is, unfortunately, very high, since direct measurements are not used. However, comparisons presented here will be against Kapton, and the influence of sputter yields of the other materials in the simulation is minimal.

For the two existing plasma simulations, PRESCRIBED_PLUME and RAY, redeposition is calculated by ray tracing. The sputtered flux is distributed as the cosine of the off-normal angle and projected from the sputtering elements to all other viewable surface elements. More detailed models will replace this simple model in the future.

Sputtered material may be deposited on surfaces exposed to the ion beam. There, the deposited material may be re-

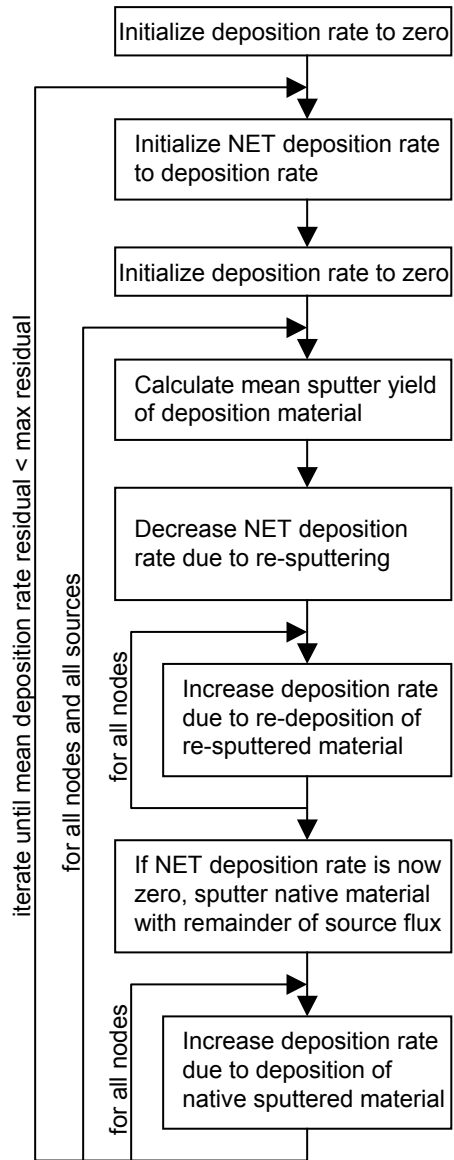


Fig. 4. Flow diagram for the re-sputtering algorithm.

sputtered onto other surfaces, as shown in Fig. 3. This re-sputtering process may be very important because, for certain geometries, it may influence the type and thickness of re-deposited material on a large percentage of the surface.

For the two existing plasma simulations, PRESCRIBED_PLUME and RAY, an algorithm has been developed to model re-sputtering, and iteratively calculate net sputtering and deposition rates at all surface nodes. Fig. 4 shows a flow description of the algorithm.

The algorithm starts by zeroing the total deposition rate of all materials to all nodes. Then, it calculates the new total deposition rate at each node for each material type. On the second and subsequent iteration, the algorithm again

```

# coliseum.in
#
# Load the Chamber 6 geometry,
# superimpose the 200W HET plume
# calculation by SAIC, calculate
# the flux and net sputtering using
# ray tracing, and save the
# results in Tecplot format.
#

component load component.txt

material load material.txt mat mat.txt

surface_load ANSYS Chamber6.ANS

prescribed plume load 2DCIRC
plume SAIC 200W.dat 0.0 0.0 0.0 0.0 0.0 1.0

ray DEPOSIT 40

surface save TECPLOT Chamber6.dat
FLUXNORMAL.XE+ SPUTTERRATE

```

Fig. 5 Sample COLISEUM command file

calculates the new total deposition rate, but takes into account the deposition from the previous iteration. This process is repeated until equilibrium, defined as the point at which the mean residual of the net deposition rate falls below some low value that the user selects.

Specifically, deposition from the previous iteration is taken into account by first storing the total deposition rate from the last iteration into a “net” deposition rate variable. As the various sputtering sources (such as ion beams) are considered, this net deposition rate is successively depleted. If and when the net deposition rate becomes zero at a given node, the algorithm begins depleting the native material.

By “depleting”, what is meant is that the surface deposition rate is decreased. Once all of the deposition flux has been depleted, depletion refers to increasing of the local native material sputter rate. In both cases, the sputtered material is projected to all other nodes as redeposition (in the case of deposited material) or deposition (in the case of native material sputtering). When material is projected to all other nodes, the total deposition rate is increased by the appropriate amount in accordance with the cosine sputtering law mentioned earlier.

One key assumption is that the sputter yield of the “composite” deposition material, which may be made up of many different materials, is the mean of the arriving material sputter yields, weighted by their molecular fluxes:

$$\bar{Y} = \frac{\sum_k Y_k \Gamma_{D,k}}{\sum_k \Gamma_{D,k}} \quad (2)$$

Above, Y is the sputter yield, and Γ_D is the normal component of the deposition molecular flux, and k is the index of the arriving material. When re-sputtering the deposited material,

the above assumption requires that the re-sputtered flux of each material be:

$$\Gamma_{R,k} = \bar{Y} \Gamma_S \frac{\Gamma_{D,k}}{\sum_k \Gamma_{D,k}} \quad (3)$$

Where Γ_S is the flux of source particles normal to the surface. This ensures material conservation and preserves the ratio of constituents of the composite deposition material.

User Interface

The user enters commands via a COLISEUM input file. The commands are executed sequentially as they appear in the input file. Each command may have some number of parameters separated by spaces or commas. A sample input file is shown in Fig. 5.

Geometry definition typically takes approximately 6 hours for medium-complexity geometries. Typical run times for low-fidelity cases (using PRESCRIBED_PLUME or RAY) take approximately 20 minutes on a 2 GHz Intel Pentium 4 workstation. Once more detailed physics are incorporated with plasma algorithms such as PIC-DSMC, run times are expected to be between 20 minutes and 20 hours, depending on the level of fidelity and on the initial conditions.

This illustrates a key feature of COLISEUM. From scratch, a user can define a complete three-dimensional problem, and generate a first order solution all in less than one workday. Then, for higher fidelity solutions, the problem does not have to be redefined. Since the plasma simulation modules are interchangeable, a higher-fidelity algorithm may be immediately started for an overnight run.

Results and Discussion

For the results presented here, COLISEUM, runs were executed for two cases: A) an HET firing inside a laboratory vacuum chamber, and B) a fictitious geosynchronous satellite with an HET firing in the north direction (as if for stationkeeping). Case A is an attempt to validate the sputtering models, and case B is a generalized application to a fictitious spacecraft problem. In case A, RAY was used with HET source based on Faraday cup measurements taken at AFRL. In case B, PRESCRIBED_PLUME, was used to superimpose a previously calculated plume expansion model onto the surface geometry. The plume expansion model used here was calculated for a Busek 200-Watt HET¹⁰ by SAIC using the GILBERT^{3,11} toolbox. Comparisons of this plume model with experiment can be found in a paper by Gardner et al.¹²

Case A

Results from case A are shown in Fig. 6 through Fig. 11. Fig. 8 shows the geometry of a test performed at AFRL. Inside a vacuum chamber, the Busek 200W engine was mounted horizontally on the chamber centerline. A horizontal aluminum table covered with Kapton was mounted 0.188m

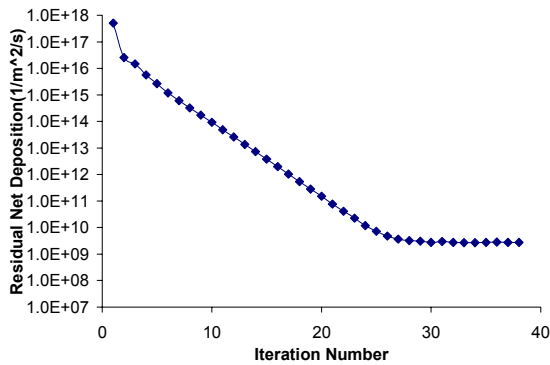


Fig. 6. Convergence of the residual of the mean net deposition rate versus iteration number for the laboratory test case.

below the engine. Samples of Kapton and other materials, each approximately 2 cm² were placed in rows on the table at varying distances from the thruster exit plane. The chamber walls were stainless steel, but a square spherical graphite panels were attached to the wall 1.36 meters from the engine face.

Before and after a 100-hour engine firing at 250V and 830mA discharge, the Kapton samples were weighed and their thickness was measured. The differences in sample mass agreed well with the differences in sample thickness (using a Kapton density of 1.42 g/cc).

Fig. 9 shows the orientation of the plume generated by the 200-Watt HET plume. Plasma density is highest near the HET exhaust, and drops off rapidly as the plume expands into the test section.

Fig. 6 shows, for case A, the convergence properties of the re-sputtering algorithm presented in the previous section. As can be seen from the figure, the mean residual of the net deposition rate decreases exponentially with the number of iterations. For geometries with around 10,000 surface elements, like case A, convergence to machine precision typically occurs after approximately 30 iterations.

Fig. 10 and Fig. 11 show the resulting net sputtering and deposition rates, respectively. The net sputtering peaks on the Kapton-covered table where the incidence angle of the ion beam is approximately 60 degrees. This is due to two effects – increased xenon ion flux at that point, and the model for Kapton sputtering yield, which also peaks at approximately 60 degrees. The net deposition rate peaks on the engine face because of the simplified flat surface model. On the table, most of the deposited graphite is “cleaned” from the surfaces by the plume. In the area behind the engine exit plane, deposition occurs on the table because ion fluxes are assumed

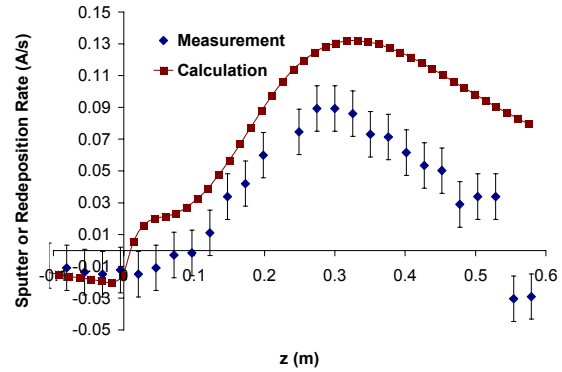


Fig. 7. Comparison between measured and calculated sputtering/deposition rates of Kapton samples. (x=0m, y=-0.188m). Negative values represent net deposition.

to be zero in this region; thus, “cleaning” does not occur there.

Fig. 7 compares the measured and calculated values of Kapton sputtering/redeposition on the table. Negative values indicate net deposition of material that was sputtered from the stainless steel walls and graphite panel. Net deposition can be seen for $z < 0.1m$ in the measurements, and $z < 0m$ in the calculation. This area is underneath the HET, and behind the plume impingement region. Therefore, very little ion flux exists to “clean” away deposited material.

Also in Fig. 7, one can see that the measured and calculated net sputtering rate of Kapton differ by up to 0.06 Angstroms per second. Some possible explanations are: a) our model for Kapton sputtering is inaccurate, b) the 200W HET plume model differs from the real case, or c) additional surface effects due to the deposition of graphite effectively harden the surface. This is an area for continued investigation.

Case B

Results from case B are shown in Fig. 12 through Fig. 15. Fig. 12 shows the geometry of a generalized geosynchronous satellite. Fig. 13 shows a cross-section of a superimposed HET plume, pointing north. Plasma density is highest near the HET exhaust, and drops off rapidly as the plume expands upward toward the solar arrays.

Sputter rate was calculated using the models presented above, and is shown in Fig. 14. The total rate of redeposition of solar array coverglass is shown in Fig. 15.

Although the net sputtering rate peaks on the radiator wing, most of the total sputtering occurs on the north solar panel and on its concentrators. This illustrates a real problem with electric propulsion on geosynchronous satellites. For north-south stationkeeping, the ideal firing direction (from a thrust efficiency standpoint) is directly north. However, the

simulations shows that long-term firing of the HET over the lifetime of a satellite in this configuration may remove a significant amount of material from the spacecraft. In reality, the solar array will be rotating to track the sun, and will not always be positioned directly in the HET plume. Furthermore, the HET would probably be tilted away from due north to reduce plume impingement. Thus, the configuration presented here can be considered a worst case.

Redeposition of sputtered solar array cover glass, shown in Fig. 15, illustrates another potential problem in using EP onboard spacecraft. During HET firing, sputtered material from the solar panels may accumulate on radiator panels, reflectors, or other sensitive surfaces. At the rates predicted here, the emissivity of the material on top (North) of the spacecraft could be changed.

Conclusions

Although still in an early stage of development, COLISEUM now can help predict ion flux and equilibrium net sputtering and deposition rate of surface materials both onboard spacecraft and in laboratory test facilities. COLISEUM's modular architecture is allowing rapid expansion of its capabilities, and giving users flexibility to design their own geometries and choose their preferential plasma simulation method.

The model presented here predicts net sputtering rate of Kapton within 0.06 Angstroms per second for the geometry tested. Some possible causes of discrepancy are a) our model for Kapton sputter yield is inaccurate, b) the 200W HET plume model differs from the real case, or c) additional surface-hardening may be taking place due to the deposition of graphite.

Additional work for the future includes further investigation of the re-sputtering process, further validation against experimental data, and construction of new plasma simulation modules that can self-consistently compute plasma expansion and interaction with surfaces.

References

- ¹Kim, V., et al., "Electric Propulsion Activities in Russia," IEPC-01-005, 27th International Electric Propulsion Conference, 2001.
- ²Boyd, I. D., "A Review of Hall Thruster Plume Modeling," AIAA-00-0466, AIAA Aerospace Sciences Conference, 2000.
- ³Gardner et al., "Hall Current Thruster Plume Modeling: A Diagnostic Tool for Spacecraft Subsystem Impact," AIAA-2001-0964.
- ⁴Mikellides, I.G., et al., "A Hall-Effect Thruster Plume and Spacecraft Interactions Modeling Package," IEPC-01-251, 27th International Electric Propulsion Conference, 2001.
- ⁵Roussel et al., "Numerical Simulation of Induced Environment, Sputtering and Contamination of Satellite due

to Electric Propulsion," Proc. Second European Spacecraft Propulsion Conf. 1997.

⁶K. Kannenberg, V. Khayms, S. H. Hu, B. Emgushov, L. Werthman, and J. Pollard "Validation of a Hall thruster plume sputter model," Paper AIAA-2001-3986, 37th Joint Propulsion Conference, 8-11 July 2001, Salt Lake City, Utah.

⁷Boyd, I. D. and Falk, M. L., "A Review of Spacecraft Material Sputtering by Hall Thruster Plumes," AIAA Paper 2001-3353, 37th Joint Propulsion Conference, Salt Lake City, Utah, 8-11 July 2001.

⁸Fife, J. M. et al., "Spacecraft Interaction Test Results of the High Performance Hall System SPT-140," AIAA-2000-3521, 36th AIAA Joint Propulsion Conference, Huntsville, Alabama, 17-19 July 2000.

⁹Rosenberg, D. and Wehner, G. K., "Sputtering Yields for Low Energy He⁺, Kr⁺, and Xe⁺ Ion Bombardment," Journal of Applied Physics, Vol. 33, 1962, pp. 1842-1845.

¹⁰V. Hruby, J. Monheiser, B. Pote, C. Freeman, and W. Connolly, "Low Power, Hall Thruster Propulsion System," IEPC-99-092, 26th International Electric Propulsion Conference, 17-21 October, 1999, Kitakyushu, Japan

¹¹Katz et al., "A Hall Effect Thruster Plume Model Including Large-Angle Elastic Scattering," AIAA-2001-3355, 37th Joint Propulsion Conference, Salt Lake City, Utah, 8-11 July 2001.

¹²Gardner et al., "Assessment of Spacecraft Systems Integration Using the Electric Propulsion Interactions Code," AIAA-2002-3667, 38th AIAA/ASME/SAE/ASEE Joint Propulsion Conference, Indianapolis, Indiana, 2002.

CASE A – Laboratory Experiment with 200W HET

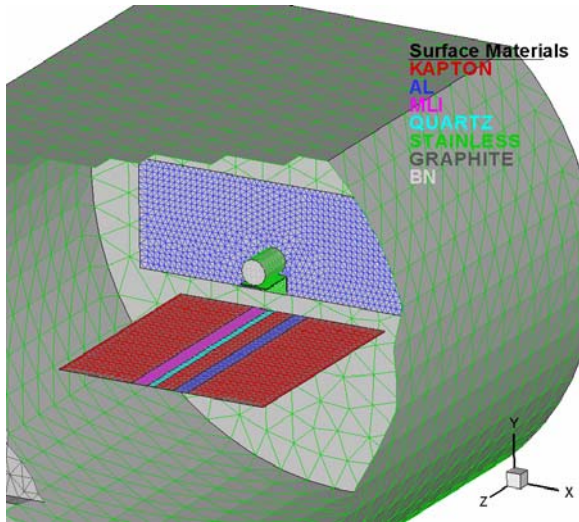


Fig. 8. Cutaway of an HET test setup showing the HET, a horizontal Kapton-covered table, and graphite panels placed on the vacuum chamber walls.

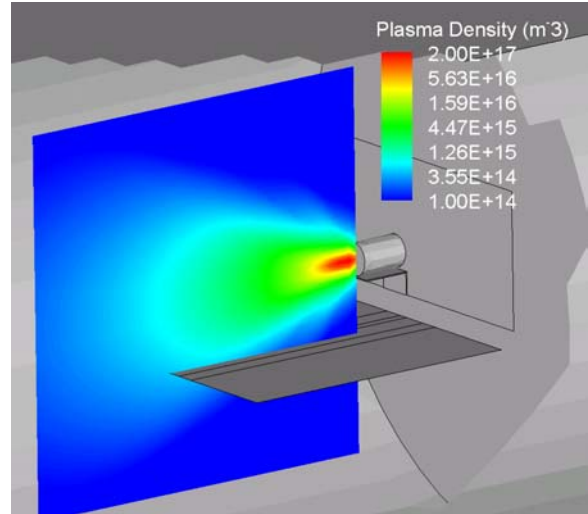


Fig. 9. Slice showing the orientation of the thruster plume and approximate plasma density values.

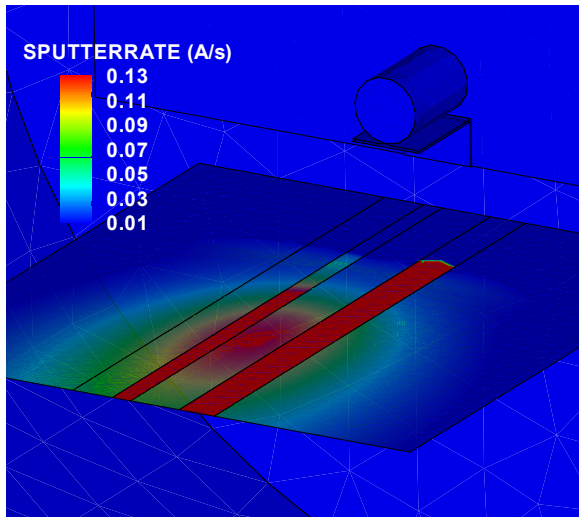


Fig. 10. Net surface sputtering rate. Negative values indicate net deposition.

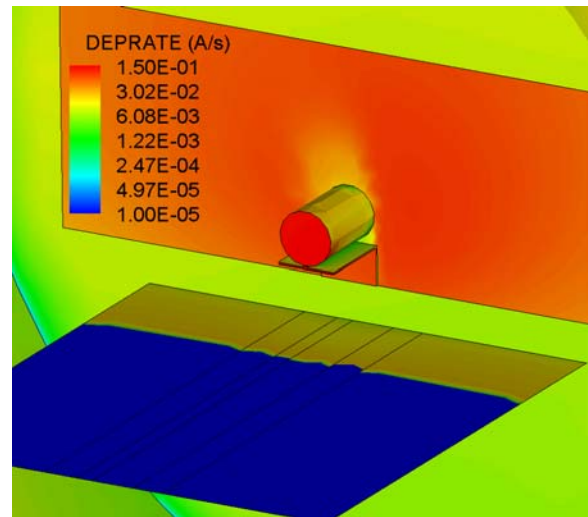


Fig. 11. Net deposition rate.

CASE B – Geosynchronous Satellite with HET for North-South Stationkeeping

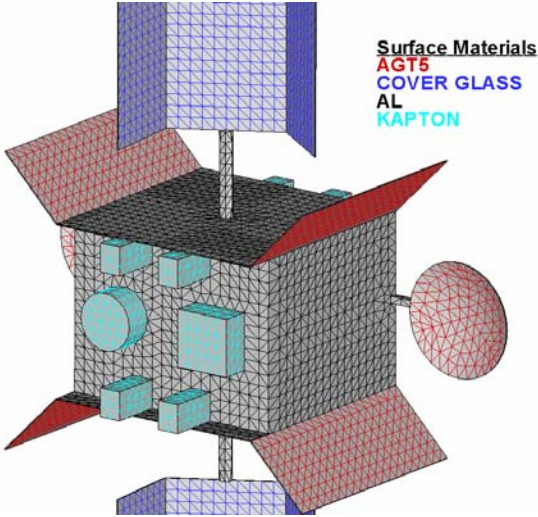


Fig. 12. Surface mesh of a geosynchronous satellite geometry with eight HETs positioned for north-south stationkeeping.

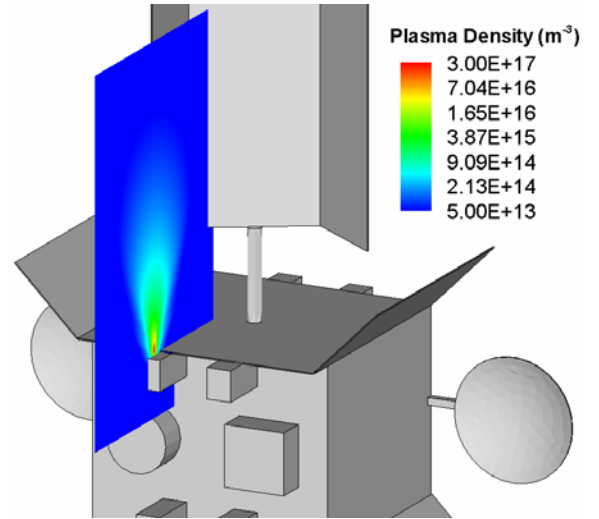


Fig. 13. Slice showing plasma density from a 200-Watt HET firing onboard a geosynchronous satellite.

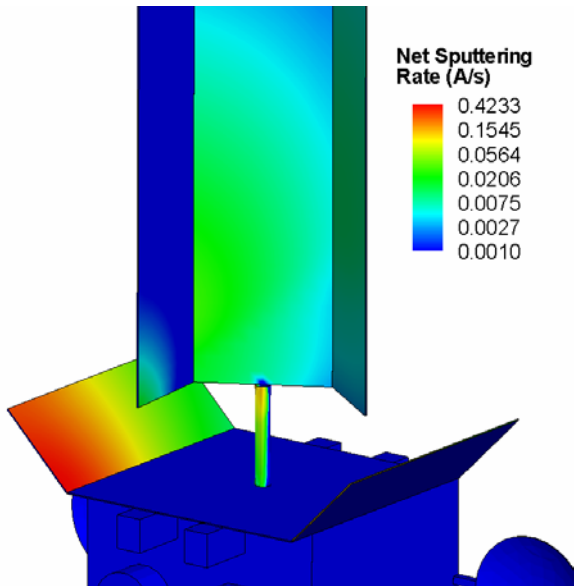


Fig. 14. Net surface sputtering rate.

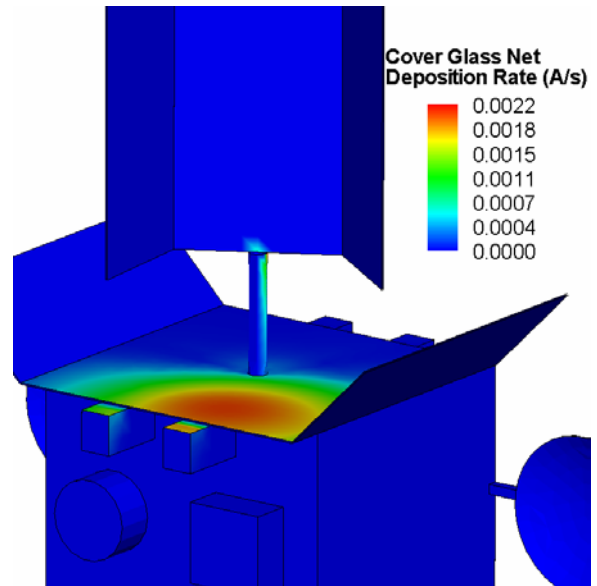


Fig. 15. Total redeposition rate of ITO from the solar array cover glass to other spacecraft surfaces due to sputtering.